Journal of Statistical Physics, Vol. 90, Nos. 5/6, 1998

Spectral Analysis of Stochastic Phase Lockings and Stochastic Bifurcations in the Sinusoidally Forced van der Pol Oscillator with Additive Noise

Shinji Doi,[1,3] Junko Inoue,[2] and Sadatoshi Kumagai[1]

Received August 17, 1997

Noise effects on the phase lockings and bifurcations in the sinusoidally forced van der Pol relaxation oscillator are investigated. Deterministic (noise-free) one-dimensional Poincaré mapping is extended to the iteration of the operator defined by a stochastic kernel function. Stochastic phase lockings and bifurcations are analyzed in terms of the density evolution by the operator. In particular, a new method which uses spectra (eigenvalues and eigenfunctions) of the operator to analyze stochastic bifurcations intensively is proposed.

KEY WORDS: van der Pol equation; relaxation oscillation; additive noise; phase locking; stochastic bifurcation; spectrum; Perron–Frobenius operator.

1. INTRODUCTION

The van der Pol oscillator[8] is a prototypical nonlinear oscillator and is widely utilized as a model of various physical, biological, and engineering systems. The oscillator presents a so-called relaxation oscillation[5] in the limit of high nonlinearity. A relaxation oscillator has two different time scales: slow and fast dynamics. Dynamics with multiple time scales are typical in biological systems, especially in neuronal systems.[4,6]

The study of the effect of an external (deterministic) forcing on the oscillator is important since a physical oscillator does not usually stand alone and is connected to the environment and/or other oscillators.

[1] Department of Electrical Engineering, Faculty of Engineering, Osaka University, Suita, 565 Japan.

[2] Department of Computer and Business, Koka Women's College, Nishikyogoku, Kyoto 615, Japan.

[3] To whom correspondence should be addressed; e-mail: doi@pwr.eng.osaka-u.ac.jp.

0022-4715/98/0300-1107$15.00/0

Oscillators also suffer noise, which may represent environmental noise or uncertainty due to the limitation of our knowledge about real systems. Thus we study the (piecewise-linearized) van der Pol relaxation oscillator in the presence of both an external periodic signal and noise. Recently, such a periodically forced system with noise has attracted much attention in the context of stochastic resonance,[16] while research on the effects of noise on general systems has a long history, and noisy or stochastic dynamical systems have been investigated in a wide context.[12]

Grasman and Roerdink[7] studied the van der Pol relaxation oscillator in the presence of noise and reduced the problem of examining the period of the oscillator to the analysis of the time necessary for a one-dimensional stochastic process to reach a boundary for the first time. Tateno *et al.*[14] extended this first-passage-time approach to the case of a periodic forcing. In the present paper, we develop this work[14] to study intensively the effect of noise on the phase lockings and bifurcations in the forced relaxation oscillator.

Section 2 presents the sinusoidally forced (piecewise-linearized) van der Pol oscillator with noise. The periodically forced relaxation oscillator without noise displays various phase-locking patterns and bifurcations if some control parameters such as the amplitude and/or period of the periodic forcing are changed. This system is usually analyzed in terms of the iterations of a one-dimensional return map or a Poincaré map of a "phase" variable. Section 3 defines a (stochastic) kernel function as a stochastic extension of the return map. Then the system of iterations of the deterministic return map is extended to the system of iterations of an operator defined by the kernel function. Examples of stochastic phase lockings are presented in the framework of the evolution of a probability density function (pdf) of the phase variable by the operator. Section 4 studies briefly the noise effects on bifurcation phenomena using the stationary or asymptotic pdf's generated by the operator. Section 5 proposes a new method which uses spectra (eigenvalues and eigenfunctions) of the operator to analyze the stochastic bifurcations in detail.

Stochastic dynamical systems are usually analyzed from the viewpoint of stationary or asymptotic probability distributions of some state variables, e.g., the stationary solution of the Fokker–Planck equation in a continuous-time system and the invariant density of the Frobenius–Perron operator in a discrete-time system. Recently, the more dynamic viewpoint rather than the static one has been emphasized.[11, 13] Classically, the definition of a stochastic bifurcation is based on the change of the topological shape of the stationary probability distribution and ignores the dynamic viewpoint; the definition utilizes only static information.[9] Recent development of a stochastic bifurcation theory overcomes this drawback and takes

the dynamic information of a stochastic system into account.[1, 2, 17] The system studied in the present paper, however, seems to show no stochastic bifurcation even in this sense of the new theory. Our approach of using spectra of the operator is a simple alternative to analyze a stochastic bifurcation from a dynamic point of view.

2. VAN DER POL RELAXATION OSCILLATOR

We consider a sinusoidally forced (and piecewise-linearized) van der Pol relaxation oscillator in the presence of additive noise:

$$\varepsilon \frac{dx}{dt} = f(x, y) \tag{1a}$$

$$\frac{dy}{dt} = -x + v(t) + \sigma \frac{dW(t)}{dt} \tag{1b}$$

$$f(x, y) = y - x + 5/6\{|x+1| - |x-1|\}$$

$$v(t) = A \sin\{2\pi(t/T + \theta_0)\}$$

where A, T, and θ_0 are the amplitude, the period, and the initial phase of the sinusoidal input, respectively. $W(t)$ is the standard Wiener process and $\sigma\, dW(t)/dt$ denotes a Gaussian white noise with a noise intensity σ. Note that the cubic polynomial of the original van der Pol equation is piecewise linearized for computational purposes.[14] Throughout, we consider the so-called singular limit of $\varepsilon = 0$. In this case, the van der Pol oscillator shows a relaxation oscillation.

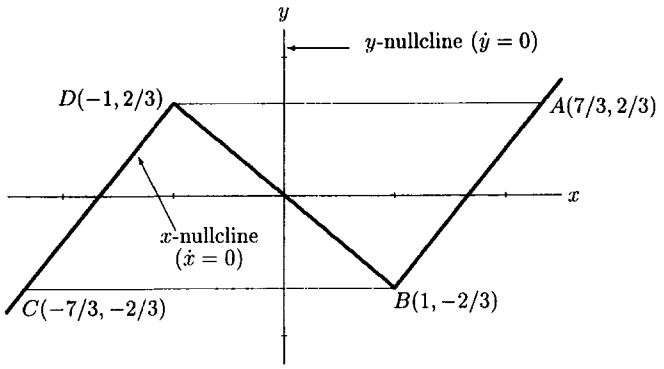

Fig. 1. The x-y phase plane of (1) in the limit of $\varepsilon = 0$ and the N-shaped x-nullcline ($\dot{x} = 0$). The y-nullcline ($\dot{y} = 0$) coincides with the y axis. The closed orbit ABCD is a limit cycle. See text for details.

Figure 1 shows the x–y phase plane of (1). In the limit of $\varepsilon = 0$, the orbit with an initial value which is not on the N-shaped x-nullcline ($\dot{x} = 0$) instantaneously jumps to the x-nullcline in the horizontal direction since the horizontal velocity $\dot{x} = f(x, y)/\varepsilon$ becomes infinite unless $f(x, y) = 0$. Thus, all orbits are considered to move on the x-nullcline and both the sinusoidal and noise terms of (1b) modulate the velocity of the orbit along the x-nullcline. On the right (left) branch of the N-shaped x-nullcline, an orbit moves toward the point B (D, resp.). At the point B (D), the orbit instantaneously jumps to the point C (A, resp.), since we consider the limit of $\varepsilon = 0$. This limit is called singular, since orbits are not differentiable at such jump points. The parallelogram ABCD is a limit cycle to which every orbit of (1) approaches asymptotically.

3. STOCHASTIC KERNEL AND MARKOV OPERATOR

Consider the noise-free ($\sigma = 0$) case and a Poincaré or return map as follows. Suppose that an orbit starts at the point A of the x–y phase plane with an initial "phase" θ_0 of the sinusoidal input and that the point returns to the point A again after a time t. Then the phase of the sinusoidal input is changed from θ_0 to θ_1:

$$\theta_1 = p(\theta_0) \stackrel{\text{def}}{=} t/T + \theta_0 \qquad (\text{mod } 1)$$

Phase lockings of the noise-free case are usually analyzed by this return map $p(\theta)$ and by the one-dimensional mapping:

$$\theta_{n+1} = p(\theta_n), \qquad n = 0, 1, 2, \ldots \tag{2}$$

The sequence $\{\theta_n\}$ generated by this one-dimensional discrete-time dynamical system will be referred to as the orbit of (2) in the same way as the orbit of (1) unless any confusions might occur. Generally, in the case of m:n locking, the orbit or sequence $\{\theta_n\}$ asymptotically approaches to an n-periodic orbit (sequence):

$$\theta^{(0)}, \theta^{(1)}, \ldots, \theta^{(n-1)}, \theta^{(0)}, \ldots$$

We extend the deterministic map to the case with noise in the following way. In the noisy case, both variables θ_0 and θ_1 fluctuate owing to noise and thus are random variables Θ_0 and Θ_1, respectively. Define a kernel function $g(\theta_0, \theta_1)$ using a conditional probability density function:

$$g(\theta_0, \theta_1)\, d\theta_1 = \Pr\{\theta_1 \leqslant \Theta_1 \leqslant \theta_1 + d\theta_1 \mid \Theta_0 = \theta_0\} \tag{3}$$

The function $g(\theta_0, \theta_1)$ can be calculated numerically without simulations of the stochastic differential equations (1).[14]

Figure 2a shows an example of the return map $p(\theta)$ and its orbit $\{\theta_n\}$. The graph of $p(\theta)$ intersects a diagonal line at two points (indistinguishable in this figure) and the lower intersection point θ^* is a stable fixed point of (2). Thus an orbit $\theta_0, \theta_1, \ldots$ with any initial phase θ_0 asymptotically converges to this fixed point θ^*, which shows that a 1:1 phase locking occurs. Figure 2b shows the kernel function g which corresponds to the deterministic map of Fig. 2a. The function g takes relatively high values along the graph of the map p. Thus g can be considered as the stochastic extension of the return map. The heights and widths of the peaks of g depend on the values of (θ_0, θ_1) and thus we can see that the effects of blurring of the deterministic map by noise are not uniform.

Using the kernel function g, we extend the system (2) to the noisy case. Let S denote a unit interval $[0, 1]$ and $\mathscr{D}$ the set of absolutely integrable nonnegative functions with a unit L^1 norm on S. A function which belongs to $\mathscr{D}$ is called a probability density function (pdf) or simply a density function. A (Markov[11]) operator $\mathscr{P}$ on $\mathscr{D}$ is defined by

$$\mathscr{P}h(\theta) = \int_S g(\theta_0, \theta)\, h(\theta_0)\, d\theta_0, \qquad h \in \mathscr{D} \tag{4}$$

Let $h_0(\theta) \in \mathscr{D}$ denote the probability density function of the initial phase Θ_0 when an orbit starts at the point A of the x–y phase plane. Then the

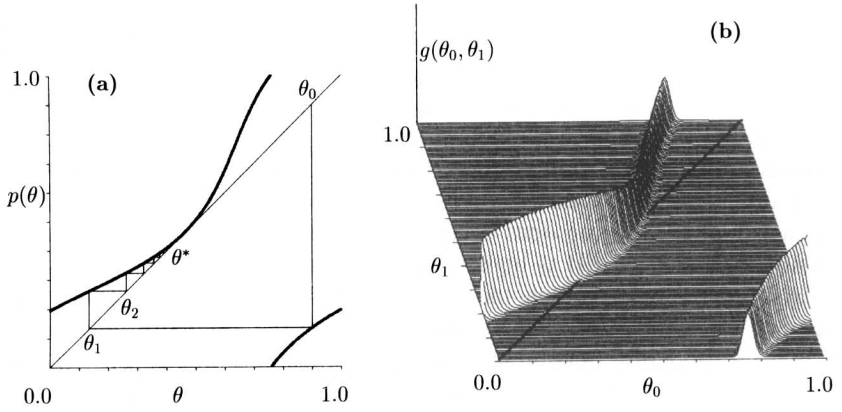

Fig. 2. (a) Poincaré or return map $p(\theta)$ (thick curve) and its orbit $\{\theta_n\}$ (thin lines). $A = 0.3$, $T = 1.5$. The orbit $\theta_0, \theta_1, \ldots$ asymptotically converges to a fixed point θ^* which corresponds to a 1:1 phase locking. (b) Stochastic kernel function $g(\theta_0, \theta_1)$ which corresponds to the deterministic map of part (a). $\sigma = 0.03$.

density function of Θ_1 when the orbit returns to the point A again is obtained by $h_1(\theta) = \mathscr{P}h_0(\theta)$. Thus, the deterministic mapping (2) is extended to the system

$$h_{n+1}(\theta) = \mathscr{P}h_n(\theta), \qquad n = 0, 1, 2, \ldots \tag{5}$$

Note that we investigate the asymptotic behavior of the sequence $\{h_n(\theta)\}$ of probability density functions rather than the sequence $\{\theta_n\}$.

Let us list several preliminary definitions.[11] A function $h^*(\theta)$ is called the *invariant density* function of an operator $\mathscr{P}$ if the relation $\mathscr{P}h^* = h^*$ holds. The invariant density is *asymptotically stable* if for any initial density function $h_0 \in \mathscr{D}$

$$\lim_{n \to \infty} \| \mathscr{P}^n h_0 - h^* \| = 0$$

As is easily seen from its definition, the function g has the property

$$g(\theta_0, \theta_1) \geqslant 0, \qquad \int_S g(\theta_0, \theta_1)\, d\theta_1 = 1$$

and is called a stochastic kernel. The inequality

$$\int_S \inf_{\theta_0} g(\theta_0, \theta_1)\, d\theta_1 > 0 \tag{6}$$

is assumed to hold.[14] The operator with this property is known to have a unique asymptotically stable invariant density (see Corollary 5.7.1 of ref. 11). Thus the sequence $\{h_n(\theta)\}$ produced by the operator $\mathscr{P}$ always approaches a unique invariant density asymptotically as $n \to \infty$.

Figure 3 shows examples of the evolution (or sequence) of $h_n(\theta)$. Figure 3a corresponds to the deterministic 1:1 phase locking (Fig. 2). The uniform initial density function $h_0(\theta)$ changes its shape and approaches an invariant density function h^* ($\approx h_{30}$) with one sharp peak, which shows that a 1:1 phase locking does occur in a stochastic sense. The peak of the density functions $\{h_n(\theta)\}$ is highest near $n = 7$ and is relatively lower in the invariant density h^*, which means that a large initial phase fluctuation becomes small quickly after several cycles of the oscillator and finally becomes a moderate fluctuation. This phenomenon is due to the fact that the peaks of the kernel function $g(\theta_0, \theta_1)$ near $\theta_0 = \theta_1 = \theta^*$ are lower than other peaks (cf. Fig. 2).

Figure 3b corresponds to the coexistence of two 2:1 lockings in which the deterministic map $p(\theta)$ has two stable fixed points (attractors) and the forced van der Pol oscillator shows two different modes of 2:1 phase

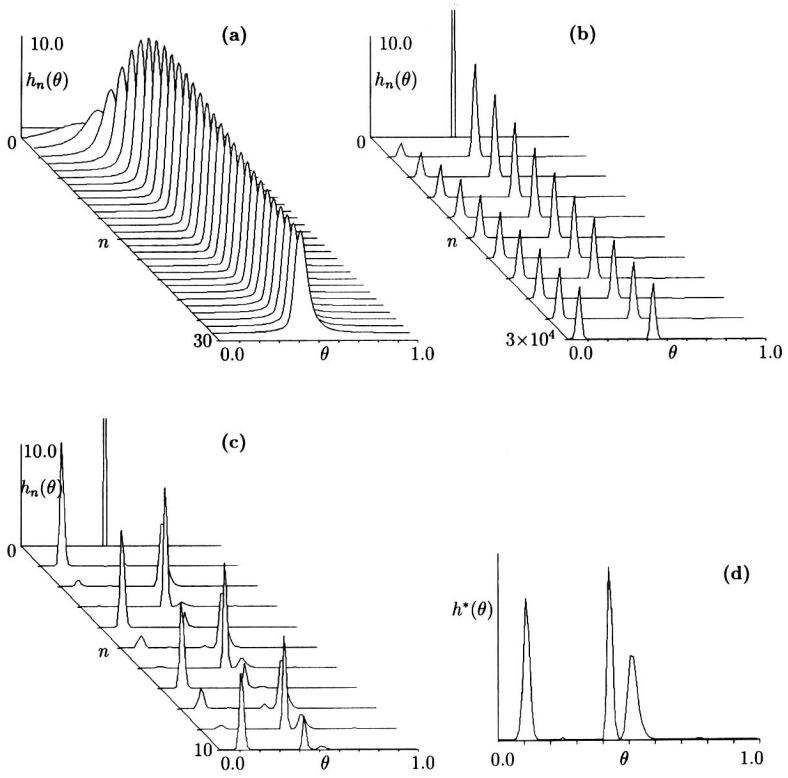

Fig. 3. Examples of density evolution (sequence) $\{h_n(\theta)\}$. (a) 1:1 phase locking. $A=0.3$, $T=1.5$, $\sigma=0.03$. A uniform initial density function evolves to an invariant density function $h^* \approx h_{30}$. (b) Coexistence of two 2:1 lockings. $A=1.5$, $T=0.85$, $\sigma=0.02$. (c) Density evolution $\{h_n(\theta)\}$ and (d) its invariant density $h^* \approx h_{200}$ of a stochastic 5:3 phase locking. $A=2.0$, $T=0.85$, $\sigma=0.02$.

lockings, depending on its initial values (see Fig. 4). The initial density with a sharp peak near one of the fixed points does not change its shape much by the operator and evolves slowly to an invariant density with two peaks. This slow change corresponds to the slow transition between the two attractors caused by noise.

Figure 3c is also an example of the density sequence in the case of stochastic 5:3 phase locking. In the corresponding deterministic case, the map $p(\theta)$ has a stable 3-periodic orbit with different three phases. The initial density function $h_0(\theta)$ has a high mode near $\theta=0.42$, which is one of the three phases to which the oscillator is locked in the noise-free case. The functions h_1 and h_2 have a high mode near the other two of the three phases. This sequence seems to vary initially with period 3, but finally

converges to an invariant density function (Fig. 3d) with three sharp peaks, which shows that a 5:3 locking occurs in a stochastic sense.

Note that there is a big difference between the convergence speed to an invariant density in Fig. 3b and Figs. 3c, d, although noise intensity is same in both cases.

4. DETERMINISTIC AND STOCHASTIC BIFURCATION DIAGRAMS

Patterns of deterministic phase lockings depend on both the amplitude and the period of the sinusoidal input. One phase-locking pattern is considered to bifurcate from the other phase-locking pattern as a (bifurcation) parameter is changed. Figure 4 shows a deterministic bifurcation diagram of the return map p for the noise-free ($\sigma = 0$) case with a bifurcation parameter A and shows how the asymptotic value(s) of the sequence $\{\theta_n\}$ change depending on the input amplitude A.

The period of the sinusoidal input is fixed as $T = 0.85$ and is about half of the intrinsic period of the van der Pol oscillator [$\ln(7/3)^2 \approx 1.69$]. So, for a wide range of the amplitude ($0.3 < A < 1.8$), 2:1 phase lockings occur (two cycles of the input synchronize with one cycle of the oscillator). In this range of A, two points are plotted and each of two points corresponds

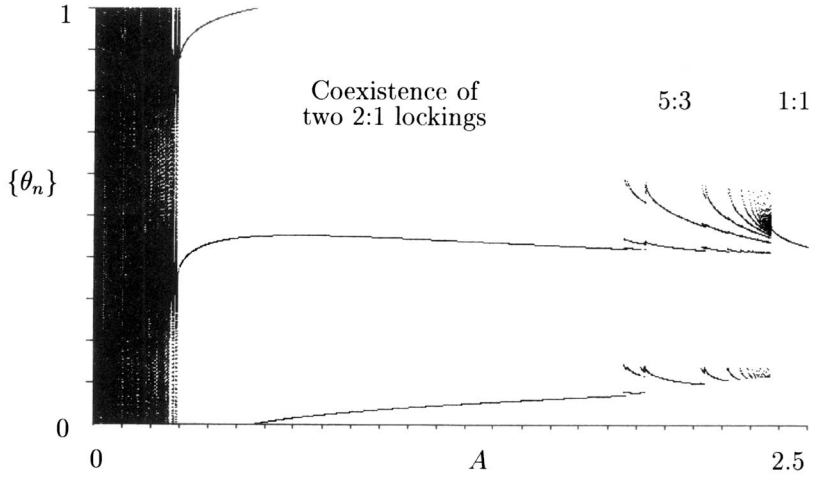

Fig. 4. Deterministic bifurcation diagram of the return map $p(\theta)$. The bifurcation parameter is the amplitude A rather than the period T, which is fixed to $T = 0.85$. Asymptotic sequences $\{\theta_n\}$, $n = 101,\ldots, 600$, produced by (2) were plotted for each of 600 equally spaced A values on the interval [0, 2.5].

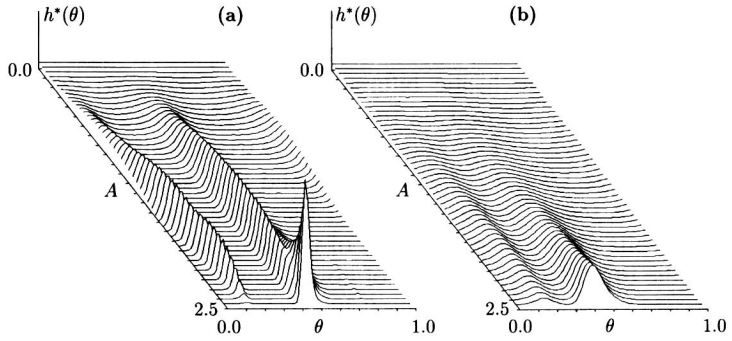

Fig. 5. Stochastic (invariant density) bifurcation diagrams. $T=0.85$. Invariant densities $h^*(\theta)$ were plotted for each of 50 equally spaced A values on the interval $[0, 2.5]$ for two different noise intensities: (a) $\sigma=0.05$ (b) $\sigma=0.2$.

to the stable fixed point (1-periodic orbit) of the mapping (2). Namely, two different patterns of 2:1 phase lockings coexist; the pattern depends on both the initial phase of the input and the initial state of the oscillator. If the value of A is changed, then various phase-locking patterns bifurcate. For example, three points are plotted when $A=2.0$. These points constitute the 3-periodic orbit of the one-dimensional mapping (2). If A is large enough ($A>2.4$), one cycle of the input can synchronize with the one cycle of the oscillator although the intrinsic periods differ by a factor of two.

Figure 5 is a stochastic or density bifurcation diagram which corresponds to the deterministic one (Fig. 4). Invariant density functions are plotted with various values of A for two different noise intensities (a) $\sigma=0.05$ and (b) $\sigma=0.2$. In Fig. 5a, corresponding to the deterministic bifurcation diagram, the peaks and the shape of the invariant density change as the bifurcation parameter A varies. In particular, in the range of $1.8<A<2.4$, the invariant densities have several peaks and complicated shapes.

In the case of large noise (Fig. 5b), the stochastic bifurcation diagram is very simple; the invariant densities have at most two peaks. The shapes of the invariant densities do not depend on the amplitude A; only the heights of the two peaks depend on A. Thus, as expected, noise washes out the dependence of the density shapes (the number of peaks) on the amplitude of the input.

In deterministic dynamical systems, the word "bifurcation" means qualitative change (number, stability) of the solutions of a system. As stated above, the equation

$$\mathscr{P}h^*=h^*$$

which the invariant density satisfies always has a "unique" asymptotically "stable" solution and thus no bifurcation of this equation occurs in such a sense. So what is a stochastic bifurcation? One (classical) definition of stochastic bifurcation is based on the "qualitative" change of the shape of the invariant density.[1,9] For example, the invariant densities change their shape in the range $1.9 < A < 2.4$ of Fig. 5a and thus stochastic bifurcations do occur in this sense. In the vicinity of the value $A = 0.29$ of Fig. 4, two 1-periodic orbits (2:1 phase lockings) of the mapping (2) bifurcate from a quasiperiodic orbit. In the presence of noise, however, the density functions always have two peaks around $A = 0.29$ (cf. Fig. 5a); the densities do not change their shape. So, in the presence of noise, we cannot see any stochastic bifurcations of a 2:1 phase locking.

Note that the recent mathematical theory[1,2] defines the stochastic bifurcations based on the existence of multiple invariant measures rather than the qualitative change of the shape of the invariant density. As stated above, we can see no bifurcations of the present system also in the sense of this new definition. Thus we will give an alternative approach which analyzes the stochastic bifurcations of the noisy van der Pol oscillator [or the system (5)] in the next section.

5. SPECTRAL ANALYSIS OF STOCHASTIC BIFURCATIONS

5.1. Eigenvalues and Eigenfunctions of the Operator $\mathscr{P}$

The linear operator $\mathscr{P}$ has all the information about the dynamics of the forced van der Pol oscillator (1) in the limit case of $\varepsilon = 0$. Numerically, this operator $\mathscr{P}$ (kernel g) is discretized and is expressed by a matrix (the density functions $\{h_n(\theta)\}$ are vectors then). This section analyzes the spectral properties (eigenvalues and eigenfunctions) of the matrix numerically. Note that we have done several numerical computations with different discretization sizes of the operator and confirmed that the following numerical results do not depend on the discretization size.

The operator $\mathscr{P}$ is positive (all elements) and is a stochastic matrix (the sum of every column is unity). Many spectral properties are known about such a positive (or nonnegative) matrix (theorem of Perron–Frobenius) and are summarized as follows[3]:

(i-a) An irreducible nonnegative (stochastic) $n \times n$ matrix A has a real eigenvalue 1 which is a simple root of the characteristic equation, and the moduli of other eigenvalues do not exceed 1.

(i-b) The "maximal" eigenvalue 1 has a positive eigenvector and there are no other (linearly independent) nonnegative eigenvectors.

(i-c) If A has k eigenvalues $\lambda_1 = 1, \lambda_2, ..., \lambda_k$ of modulus unity, these numbers are all distinct roots of $\lambda^k - 1 = 0$ and the whole spectrum $\lambda_1 = 1$, $\lambda_2, ..., \lambda_n$ of A is invariant under a rotation by the angle $2\pi/k$ of the complex plane.

(ii) Moreover, if all elements of A are positive, the maximal eigenvalue 1 exceeds the moduli of all other eigenvalues.

The operator $\mathscr{P}$ with small noise is practically considered to be a nonnegative matrix (some elements might be zero practically), although theoretically it should be positive. So it is useful to keep properties of both nonnegative matrices (i) and positive matrices (ii) in mind.

First we note that the eigenfunction (eigenvector) which belongs to the maximal eigenvalue 1 is the invariant density function h^* of the operator $\mathscr{P}$ and that the eigenvalue with largest modulus other than 1 governs the convergence speed of the sequence $\{h_n\}$ to this invariant density.

Figure 6 shows examples of the whole spectra (eigenvalues) of operators $\mathscr{P}$ with different values of A. In all figures, we can see that the operator has a unique maximum eigenvalue 1. Figure 6a corresponds to the deterministic (noise-free) quasiperiodic case (cf. Fig. 4). We can see many complex eigenvalues between zero and unity eigenvalues. Figures 6b and 6c correspond to the deterministic 2:1 phase locking. Comparing Figs. 6a–6c, we can see that eigenvalues change their values from complex to real in order of the modulus as the value of A increases, which may represent a bifurcation from quasiperiodic to 2:1 phase locking in a stochastic sense. Note that Fig. 6c corresponds to the density evolution of Fig. 3b and the second largest eigenvalue of this case is very close to 1, although we cannot distinguish this in this figure. Thus in Fig. 3b the convergence to the invariant density is very slow. Figure 6d corresponds to the deterministic 5:3 phase locking [3-periodic orbit of (2)]. We can see that the whole spectrum is roughly invariant under an angle $2\pi/3$ rotation of the complex plane, which is a sign of a stochastic 5:3 phase locking.

In the following, λ_i denotes the ith eigenvalue in the order of the modulus and $e_i(0)$ the corresponding eigenfunction; $\lambda_1 = 1$, and e_1 is an invariant density h^*. Note that λ_i, $i \geqslant 2$, may be complex and any eigenfunctions e_i, $i \geqslant 2$ (real part $\Re e_i$ and imaginary part $\Im e_i$ if λ_i is complex) other than e_1 cannot be nonnegative;[3] the functions take both positive and negative values. If we denote the eigenvalues as $\lambda_i = r_i \exp(2\pi j\omega_i)$ with imaginary unit j, we have

$$\begin{aligned}\mathscr{P}^k e_i &= \mathscr{P}^k(\Re e_i + j\,\Im e_i) = r_i^k e^{2\pi jk\omega_i}(\Re e_i + j\,\Im e_i), \qquad k = 1, 2, ... \\ &= r_i^k\{\cos(2\pi k\omega_i)\,\Re e_i - \sin(2\pi k\omega_i)\,\Im e_i\} \\ &\quad + jr_i^k\{\cos(2\pi k\omega_i)\,\Im e_i + \sin(2\pi k\omega_i)\,\Re e_i\}\end{aligned}$$

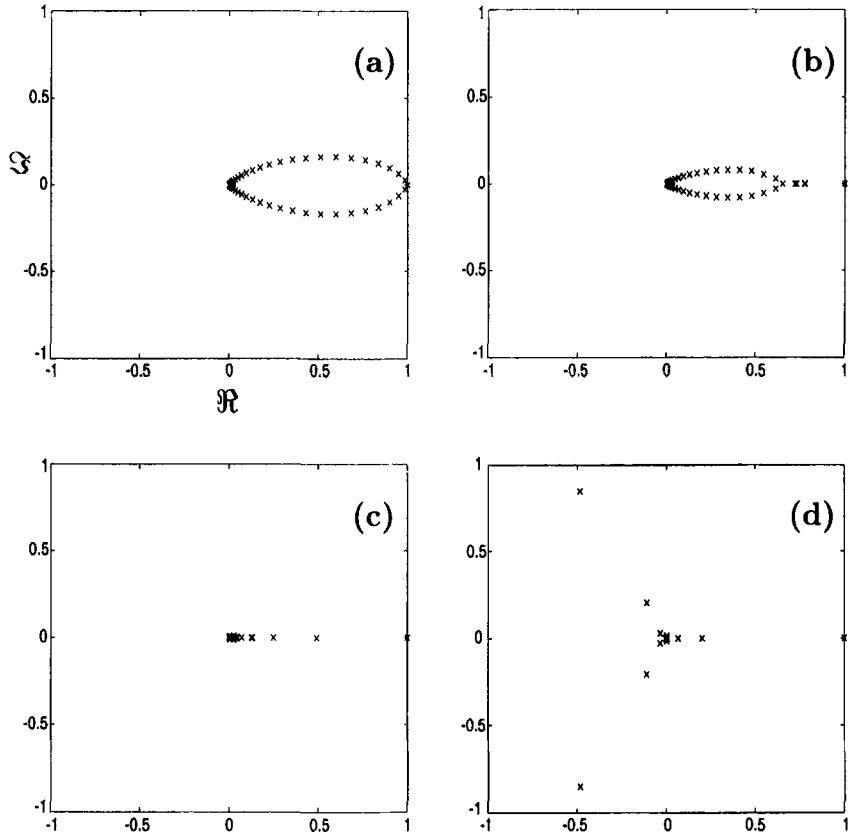

Fig. 6. Examples of spectra (eigenvalues) of the operator $\mathscr{P}$. $T=0.85$, $\sigma=0.02$. (a) $A=0.28$, quasiperiodic case. (b) $A=0.6$, 2:1 locking case. (c) $A=1.0$, 2:1 locking case. (d) $A=2.0$, 5:3 locking case. The abscissa and the ordinate are the real and imaginary parts of the eigenvalues, respectively.

Thus we have

$$\mathscr{P}^k \Re e_i = r_i^k \{\cos(2\pi k\omega_i)\, \Re e_i - \sin(2\pi k\omega_i)\, \Im e_i\} \tag{7a}$$

$$\mathscr{P}^k \Im e_i = r_i^k \{\cos(2\pi k\omega_i)\, \Im e_i + \sin(2\pi k\omega_i)\, \Re e_i\}, \qquad k=1,2,... \tag{7b}$$

If $k\omega_i$ is integer, both real and imaginary parts are invariant under $\mathscr{P}^k$ with an amplitude decay r_i^k.

Figures 7a and 7b show e_1 and e_2 (resp.), which correspond to Fig. 6c (2:1 locking). In this case, the corresponding deterministic map $p(\theta)$ has two coexisting stable fixed points (attractors) denoted by θ^* and θ^{**}. The

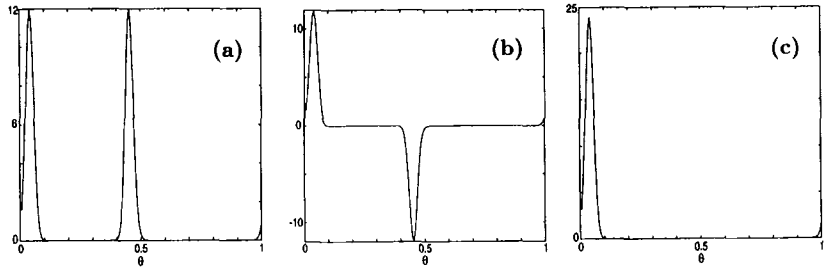

Fig. 7. Eigenfunctions of the operator $\mathscr{P}$: 2:1 phase locking. $A=1.0$, $T=0.85$, $\sigma=0.02$. (a) The first eigenfunction (invariant density) $e_1(\theta)$. (b) The second eigenfunction $e_2(\theta)$. (c) The linear combination $e=e_1+\mu e_2$.

first eigenfunction (invariant density) e_1 of Fig. 7a has two sharp peaks around the two fixed points. The second eigenfunction e_2 of Fig. 7b has positive and negative peaks around the two fixed points. Comparing Fig. 7a with Fig. 7b, we can choose a real number μ so that the linear combination $e \equiv e_1 + \mu e_2$ could become a probability density function with one sharp peak around the fixed point θ^* (see Fig. 7c). Then $\tilde{e} \equiv e_1 - \mu e_2$ has one sharp peak around the other fixed point θ^{**}. As stated above, since $\lambda_2 \approx 1$, the density function e (and $\tilde{e}$) is roughly invariant under the application of the operator $\mathscr{P}$:

$$\mathscr{P}e = e_1 + \lambda_2 \mu e_2 \approx e_1 + \mu e_2 = e$$

which corresponds to the fact that the fixed point θ^* is stable, although the density e converges to the invariant density after many iterations of the operator:

$$\mathscr{P}^n e = e_1 + \lambda_2^n \mu e \to e_1, \qquad n \to \infty$$

Figures 8a–8c show the eigenfunctions e_1, $\Re e_2$, and $\Im e_2$ (resp.) of the 5:3 locking (cf. Fig. 6d). In the corresponding deterministic case, the map $p(\theta)$ has a stable 3-periodic orbit $\theta^{(0)}$, $\theta^{(1)}$, $\theta^{(2)}$ such that

$$p(\theta^{(i)}) = \theta^{(i+1) \pmod 3}, \qquad i = 0, 1, 2$$

We can choose real numbers μ_1 and μ_2 so that a function $e \equiv e_1 + \mu_1 \Re e_2 + \mu_2 \Im e_3$ could be a density function with one sharp peak around $\theta^{(0)}$. If we define

$$\tilde{e} \equiv \mathscr{P}e, \qquad \hat{e} \equiv \mathscr{P}\tilde{e} = \mathscr{P}^2 e$$

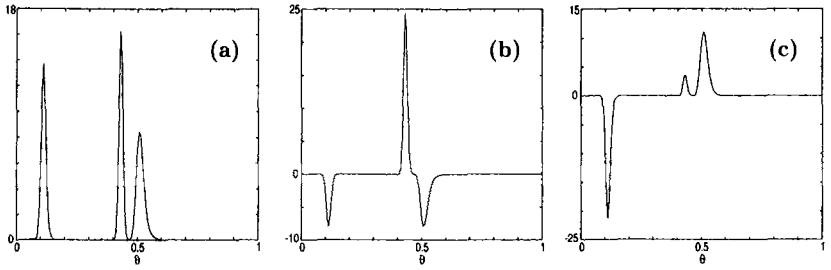

Fig. 8. Eigenfunctions of the operator $\mathscr{P}$: 5:3 phase locking. $A=2.03$, $T=0.85$, $\sigma=0.02$. (a) The first eigenfunction (invariant density) $e_1(\theta)$. (b) Real part of the second eigenfunction $e_2(\theta)$. (c) Imaginary part of $e_2(\theta)$.

then the (density) functions $\tilde{e}$ and $\hat{e}$ have one sharp peak around $\theta^{(1)}$ and $\theta^{(2)}$, respectively (strictly speaking, the functions have one sharp peak and two small peaks). The second eigenvalue $\lambda_2 = r_2 e^{2\pi j\omega_2}$ of this case is $0.95e^{0.33\times 2\pi j}$, roughly approximated by $e^{2\pi j/3}$. Thus, using Eq. (7), we have

$$\begin{aligned}\mathscr{P}^3 e &= e_1 + \mu_1 r_2^3\{\cos(6\pi\omega_2)\,\Re e_2 - \sin(6\pi\omega_2)\,\Im e_2\} \\ &\quad + \mu_2 r_2^3\{\cos(6\pi\omega_2)\,\Im e_2 + \sin(6\pi\omega_2)\,\Re e_2\} \\ &\approx e_1 + \mu_1 \Re e_2 + \mu_2 \Im e_2 \\ &= e\end{aligned}$$

which corresponds to the relation for the deterministic case:

$$p^3(\theta^{(0)}) = \theta^{(0)}$$

Thus, as is seen in Fig. 3c, the density evolves initially with a period three and finally to an invariant density. The difference of $|\lambda_2|$ from unity corresponds to the noise-induced "phase drift" from one phase to the other two of the three phases.

As demonstrated briefly in this subsection, the eigenvalues λ_i and eigenfunctions e_i with $i \geqslant 2$ possess the "dynamic" information of the operator $\mathscr{P}$, while the invariant density (first eigenfunction) e_1 possesses only "static" information. Thus the analysis of such spectra seems to be useful to study the stochastic bifurcation of the operator $\mathscr{P}$ or of the system (5), as discussed further in the following.

5.2. Spectral Bifurcation Diagram

In Fig. 9, the modulus and argument of the second, fourth, and sixth eigenvalues of the operator $\mathscr{P}$ are plotted for various A values. Note that

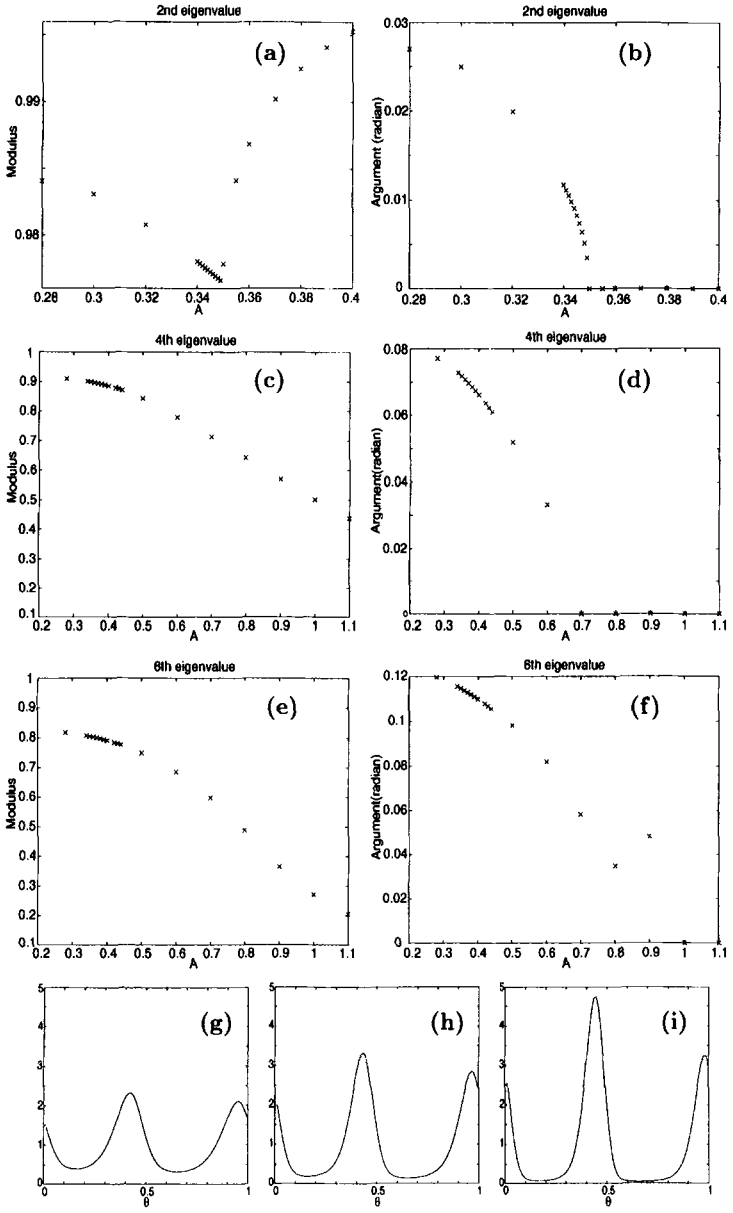

Fig. 9. Spectral bifurcation diagram (2:1 locking). (a, c, e) Moduli and (b, d, f) arguments of the second, fourth, and sixth eigenvalues are plotted, respectively, with various values of the bifurcation parameter A. Note that the range of A of (a) is different from those of (b) and (c). $T=0.85$, $\sigma=0.02$. Invariant densities are also plotted: (g) $A=0.28$, (h) $A=0.349$, (i) $A=0.4$.

a bifurcation from a quasiperiodic orbit to a 2:1 phase locking occurs in the corresponding deterministic case (cf. Fig. 4). Near $A = 0.35$, the second eigenvalue abruptly changes its value from complex to real and the modulus also abruptly changes from decreasing to increasing (see Figs. 9a and 9b). As discussed above, the real and imaginary parts of the eigenfunction of an eigenvalue $\lambda_i = re^{2\pi j\omega}$ "rotate" by $2\pi\omega$ under the application of the operator $\mathscr{P}$. If ω is rational rather than irrational, then the eigenfunction is considered to be "locked" under some iterations of the operator $\mathscr{P}$. Thus, a locking in the sense of the second eigenvalue is considered to occur at $A = 0.35$.

The fourth eigenvalue also changes its value from complex to real at a different value of A (≈ 0.7) (see Figs. 9c and 9d). So, this point is also considered to be another stochastic 2:1 bifurcation point with respect to the fourth eigenvalue. Stochastic systems, in contrast to deterministic ones, may show several modes of bifurcation of one phase-locking pattern corresponding to each eigenvalue. The modulus of the fourth eigenvalue, however, decreases monotonically, in contrast with that of the second eigenvalue. The eigenvalue with a larger modulus has a more important role in the dynamics or evolution of the densities. Thus we can say that the point of the second eigenvalue change is a major bifurcation point of a 2:1 phase locking in the stochastic sense. Note that all invariant density functions have the same topological shape (two peaks) in this parameter range (Figs. 9g–9i). So, we can observe no stochastic bifurcation in the classical sense.[1, 9]

The stochastic bifurcation of 2:1 locking is demonstrated more clearly if we plot both the second and the third eigenvalues. Figure 10a shows the moduli of both the second and third eigenvalues, which corresponds to Fig. 9. Below the stochastic bifurcation point ($A < 0.35$), both the second and third eigenvalues are complex with the same modulus and they are real above the bifurcation point ($A \geqslant 0.35$). The modulus of the second eigenvalue increases after the bifurcation, while that of the third eigenvalue decreases monotonically. Note that the graph of the arguments of both the second and third eigenvalues is just a symmetrical duplication of Fig. 9b with respect to the horizontal (A) axis. Figure 10b is the same graph as Fig. 10a for a different range $1.67 \leqslant A \leqslant 1.82$ and corresponds to the right endpoint of the A interval of 2:1 phase locking (cf. Fig. 4). The third eigenvalue decreases leftward of the bifurcation point. The decrease in magnitude of the third eigenvalue of Fig. 10b is much bigger than that of Fig. 10a.

Both the moduli and arguments of the second, fourth, and sixth eigenvalues over a different range of the bifurcation parameter A are plotted in Fig. 11. In the range of $1.98 \leqslant A \leqslant 2.04$, the sixth eigenvalue rather than the

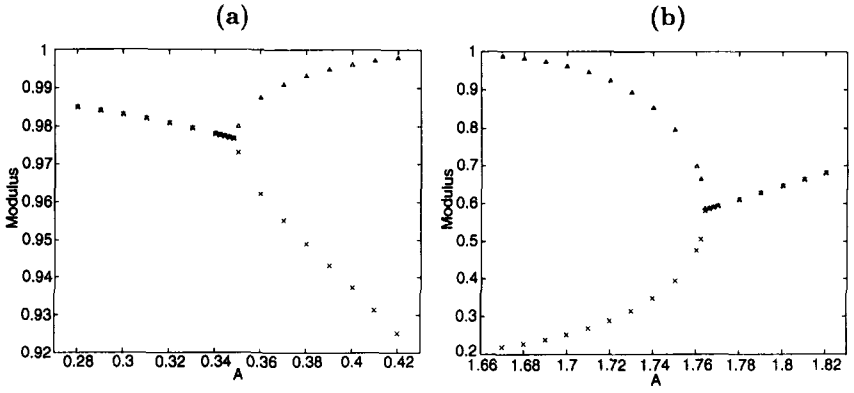

Fig. 10. Stochastic bifurcation of a 2:1 phase locking. Moduli of both the second and the third eigenvalues of the operator $\mathscr{P}$ are plotted in different ranges of A: (a) $0.28 < A < 0.42$, (b) $1.67 < A < 1.82$. $T = 0.85$, $\sigma = 0.02$. Part (a) corresponds to the left end of the A region of a stochastic 2:1 phase locking, while part (b) corresponds to the right end of the region (cf. Fig. 4).

second one abruptly changes its value to real (see Figs. 11e and 11f). This corresponds to a stochastic bifurcation of 5:3 phase locking. Note that no clear change is observed in the former (from the second to the fifth) eigenvalues, although the arguments of the second and fourth eigenvalues seem to be slightly locked to $2.09 \approx 2\pi/3$ (i.e., slightly flat) in this range of A.

The fourth eigenvalues undergo an abrupt change in the range $2.15 \leqslant A \leqslant 2.19$. This corresponds to the deterministic (noise-free) case of two coexisting 4:2 phase lockings [coexistence of two stable 2-periodic orbits of the map $g(\theta)$]. As seen briefly in Section 5.1, each eigenvalue and eigenfunction of an operator $\mathscr{P}$ has a different dynamic role in the density evolution by the operator. Thus, the eigenvalue which makes an abrupt change may depend on the corresponding deterministic phase-locking pattern. Even a fixed phase-locking pattern, as seen in the above example of 2:1 phase locking, may show different modes of bifurcations at different values of the bifurcation parameter corresponding to different eigenvalues.

In Fig. 12, the arguments of the second eigenvalues are plotted with different noise intensities. In Fig. 12a, the arguments are plotted in the range of $A = [0.28, 0.42]$. This corresponds to the spectral bifurcation diagram of Fig. 9. The stochastic bifurcation point in the sense of our definition (the point at which the eigenvalue changes its value from complex to real) is shifted rightward as the noise intensity increases. Thus noise disturbs the phase locking; a bigger input signal is required in the presence of larger noise. In Fig. 12b the arguments are plotted in the range of

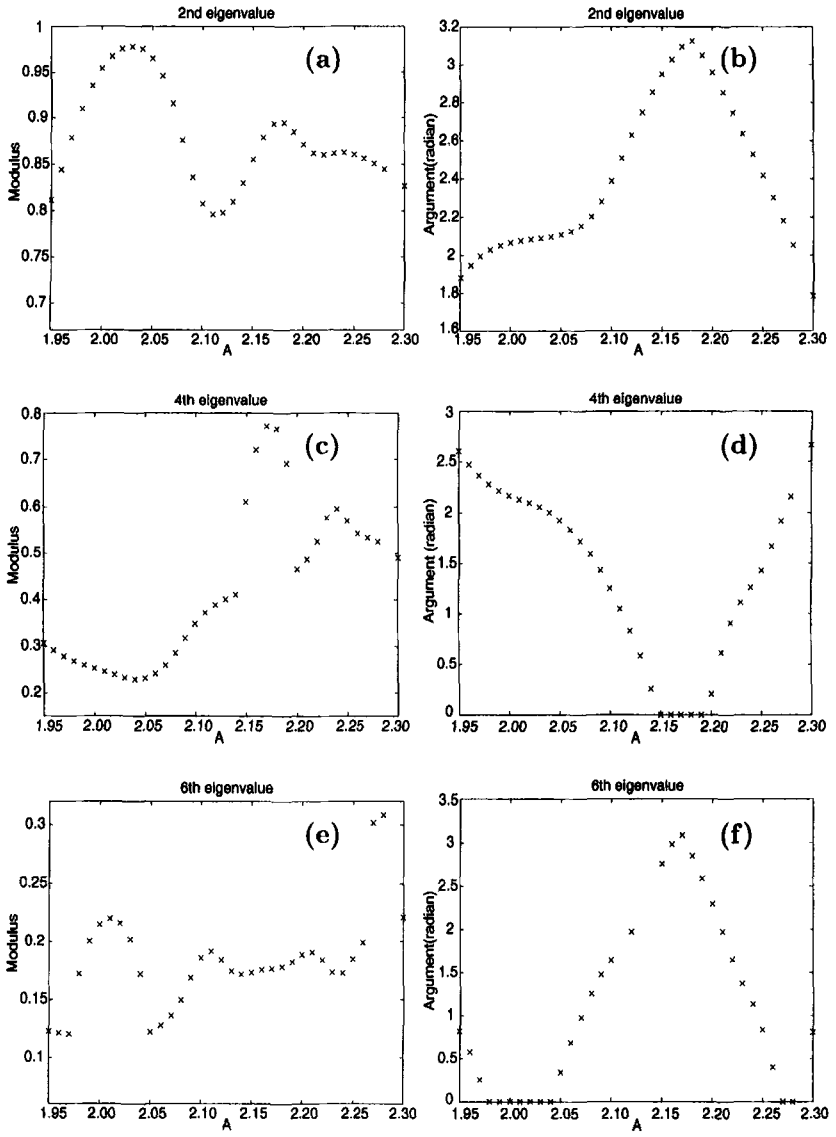

Fig. 11. Spectral bifurcation diagram (several phase lockings). (a, c, e) Moduli and (b, d, f) arguments of the second, fourth, and sixth eigenvalues are plotted, respectively, in the range of $1.95 \leqslant A \leqslant 2.3$. $T = 0.85$, $\sigma = 0.02$.

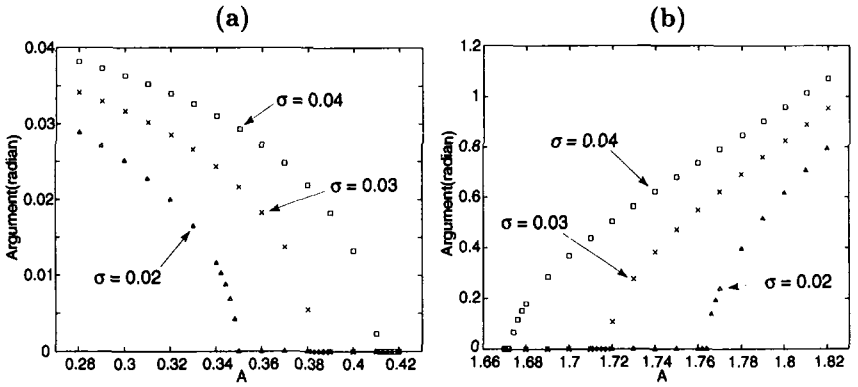

Fig. 12. Shift of stochastic 2:1 bifurcation points. Arguments of the second eigenvalues of the operator $\mathscr{P}$ are plotted with different noise intensities $\sigma = 0.02$, 0.03, 0.04, in different ranges of A: (a) $0.28 < A < 0.42$, (b) $1.67 < A < 1.82$. $T = 0.85$. The bifurcation point of part (a) corresponds to the left end of the region of a stochastic 2:1 phase locking, while that of part (b) corresponds to the right end (cf. Fig. 4). The increase of noise intensity shifts the bifurcation point rightward in (a) and leftward in (b).

$A = [1.67, 1.82]$. Figure 12a corresponds to the left endpoint of the A range of a stochastic 2:1 phase locking, while Fig. 12b corresponds to the right endpoint (cf. Fig. 4). The right bifurcation point shifts leftward differently from the left endpoint as the noise intensity increases. We can also see that the magnitude of the argument increase of Fig. 12b is much bigger than the decrease of Fig. 12a; the density evolution changes its dynamics quickly after the stochastic 2:1 bifurcation.

6. DISCUSSION

We have studied the van der Pol relaxation oscillator in the presence of both noise and sinusoidal forcing. An operator $\mathscr{P}$ is introduced as a natural extension of a deterministic (noise-free) one-dimensional return map to the presence case of noise. We can numerically compute the operator in a short time and with a high accuracy since the computation does not require numerical simulations of the stochastic differential equation (1).[14] Thus we can study very delicate phenomena caused by noise.

Using the method, stochastic phase lockings and stochastic bifurcations were analyzed; in particular, stochastic bifurcations were analyzed on the basis of spectral properties of the operator. In fact, stochastic bifurcations were clearly observed in the sense of our definition; the eigenvalues of the operator changed their values from complex to real abruptly (not smoothly) at a possible stochastic bifurcation point.

Eigenfunctions of eigenvalues with moduli less than unity have an important "dynamic" role in the density evolution by the operator $\mathscr{P}$, while the first eigenfunction or the invariant density has only a "static" role. Thus it seems reasonable to analyze stochastic bifurcations using eigenvalues other than the first one. Different eigenvalues were used, depending on the bifurcation pattern; the second eigenvalue for 2:1 phase locking and the sixth eigenvalue for 5:3 locking, etc. Eigenfunctions with different eigenvalues have different dynamic roles and it seems necessary to select the eigenvalue on a case-by-case basis, depending on the bifurcation (or phase-locking) patterns.

In contrast to deterministic dynamical systems, noisy dynamical systems may show bifurcation phenomena of several modes corresponding to second, third, fourth,... eigenvalues even in a fixed bifurcation pattern, although the larger eigenvalue has a more important role in the density evolution. In the present paper, we made only a broad discussion to demonstrate the important role of the spectra in the dynamics and in the stochastic bifurcation phenomena of the operator $\mathscr{P}$. A more rigorous discussion on the validity of our analysis of stochastic bifurcations is necessary for future research.

The operator $\mathscr{P}$, which is a stochastic extension of the one-dimensional return map, has directly (but numerically) been derived from the stochastic differential equations rather than the deterministic map $p(\theta)$. We can also consider a noisy mapping:

$$\theta_{n+1} = p(\theta_n) + \xi_n(\theta_n), \qquad n = 1, 2,...$$

where $\xi_n(\theta_n)$ denotes a (state-dependent) noise. This noisy mapping is equivalent to the forced van der Pol relaxation oscillator with noise studied in the present paper. Thus our operator is the "noisy" Frobenius–Perron operator of a noisy one-dimensional mapping.[11] If the noise is state-independent, $\xi_n(\theta_n) \equiv \xi_n$, then the noisy map is considered to be a simpler approximation of the operator. Much work has been done on such noisy maps (see ref. 10 and references therein). Our analysis method of a stochastic bifurcation is more directly and easily applicable to such noisy maps. This direction of study is now progressing.

All stochastic bifurcations presented in our examples correspond to the deterministic tangent or saddle-node bifurcations of a one-dimensional mapping. The analysis of noise effects on period-doubling bifurcations and chaos using the method would be an interesting future subject.

We have considered the case of the singular limit $\varepsilon = 0$, and thus the dynamics of the van der Pol oscillator was restricted to that along the one-dimensional limit cycle. The singular perturbation problem of considering

the $\varepsilon \neq 0$ case may be a challenging future subject. Not many studies seem to have been done for the analysis of noisy continuous-time systems (i.e., stochastic differential equations) by a stochastic return mapping, although the mapping method is typical for deterministic dynamical systems. Weiss and Knoblock[12, 15] studied a general limit cycle oscillator with small noise and derived a stochastic return map directly from a stochastic differential equation, considering dynamics both parallel and perpendicular to the limit cycle. Analysis of stochastic bifurcations of such a limit cycle oscillator also seems interesting.

REFERENCES

1. L. Arnold, Random dynamical systems, in *Dynamical Systems*, R. Johnson, ed. (Springer, Berlin, 1995).
2. L. Arnold and P. Boxler, Stochastic bifurcation: Instructive examples in dimension one, in *Diffusion Processes and Related Problems in Analysis, Vol. II: Stochastic Flows*, M. Pinsky and V. Wihstutz, eds. (Birkhäuser, 1992), pp. 241–255.
3. F. R. Gantmacher, *The Theory of Matrices*, Vol. II (Chelsea, New York, 1959).
4. L. Glass and M. C. Mackey, *From Clocks to Chaos, The Rhythms of Life* (Princeton University Press, Princeton, New Jersey, 1988).
5. J. Grasman, *Asymptotic Methods for Relaxation Oscillations and Applications* (Springer, Berlin, 1987).
6. J. Grasman and M. J. W. Jansen, Mutually synchronized relaxation oscillators as prototypes of oscillating systems in biology, *J. Math. Biol.* **7**:171–197 (1979).
7. J. Grasman and J. B. T. M. Roerdink, Stochastic and chaotic relaxation oscillations, *J. Stat. Phys.* **54**:949–970 (1989).
8. J. Guckenheimer, Dynamics of the van der Pol equation, *IEEE Trans.* **CAS-27**:983–989 (1980).
9. W. Horsthemke and R. Lefever, *Noise-Induced Transitions, Theory and Applications in Physics, Chemistry, and Biology* (Springer-Verlag, Berlin, 1984).
10. T. Kapitaniak, *Chaos in Systems with Noise* (World Scientific, Singapore, 1988).
11. A. Lasota and M. C. Mackey, *Chaos, Fractals, and Noise, Stochastic Aspects of Dynamics* (Springer, Berlin, 1994).
12. F. Moss and P. V. E. McClintock (eds.), *Noise in Nonlinear Dynamical Systems*, Vols. 1–3 (Cambridge University Press, Cambridge, 1987).
13. N. Provatas and M. C. Mackey, Asymptotic periodicity and banded chaos, *Physica* **53D**:295–318 (1991).
14. T. Tateno, S. Doi, S. Sato, and L. M. Ricciardi, Stochastic phase-lockings in a relaxation oscillator forced by a periodic input with additive noise—A first-passage-time approach, *J. Stat. Phys.* **78**:917–935 (1995).
15. J. B. Weiss and E. Knoblock, A stochastic return map for stochastic differential equations, *J. Stat. Phys.* **58**:863–883 (1990).
16. K. Wiesenfeld and F. Moss, Stochastic resonance and the benefits of noise: From ice ages to crayfish and SQUIDs, *Nature* **373**:33–36 (1995).
17. K. Xu, Bifurcations of random differential equations in dimension one, *Random Comp. Dynam.* **1**:277–305 (1993).